MULTISCALE MODELLING NANO-PLATELET REINFORCED COMPOSITES AT LARGE STRAIN

D.C. Stanier*[1], J. Ciambella[1]

[1] *ACCIS, University of Bristol, BS1 8TR Bristol, United Kingdom*
* *Corresponding Author: david.stanier@bristol.ac.uk*

Keywords: Graphene, Orientation Tailoring, Nonlinear Elasticity, Transversely Isotropic

Abstract

We study the behaviour of an incompressible particle-reinforced neo-Hookean (IPRNC) material when subjected to large plain strain deformation. The peculiarity of the model consists in the rectangular shape of the particle which yields the macroscopic response of the composites non isotropic. This is indeed the case for many reinforcements currently used in composites at all length scales: short-fibres, clays, graphene. The consequence of the anisotropic reinforcement in this model at short strain is evident in the stiffness that is observed to depend strongly on the platelet orientation; a transverse stiffening effect when the platelet is oriented perpendicular to the loading direction proves to be almost as significant as the longitudinal stiffness contribution usually considered for anisotropic reinforcements. The large strain effects of orientation are also significant and an understanding of them is relevant to a number of applications that can take advantage of the large strain non-linear response.

1. Introduction

Materials are often reinforced with fibres to improve the mechanical properties before they can be used in industrial applications, and whilst short-fibres are not able to produce the same level of reinforcement as continuous fibres, they do give a number of advantages such as increased ductility, formability and process-ability. The reinforcement these fibres provide depends primarily on its stiffness, interfacial interaction with the matrix and the specific surface area of the interface. The latter of these has led to nano-dimensioned materials being increasingly used because they provide a much larger specific interfacial area, when compared to conventional micro-sized fillers. Commonly used nano-materials include nanoclays, graphene and Carbon Nanotubes (CNTs) ; all of which have anisotropic dimensions. The anisotropy of the reinforcement has little effect on the material behaviour at the macroscale if a homogeneous dispersion is achieved, but by deliberately controlling the orientation of the reinforcement it is possible to exploit the anisotropic behaviour for use as elastomeric hinges and in devices such as actuators [1], and micro-swimmers [2].

The tailoring of microstructural reinforcement is a technique used to great effect in nature (see e.g. the design of bone [3], teeth [4] or tree structure [5]) to maximize the efficiency of materials.This is particularly relevant to devices with demanding size and weight restrictions such as micro-motors; these are micro-sized propulsion devices (often called micro-swimmers) that can

be externally actuated (e.g. magnetically) for biomedical applications (see e.g. [2]). A common approach to controlling the orientation of the reinforcement is to use magnetic fillers and align them in a strong magnetic field [6, 7, 8].

Currently there is no satisfactory model to describe the effects of an anisotropic filler from a continuum mechanics perspective using physically representable quantities. We study the behaviour of an incompressible particle-reinforced neo-Hookean (IPRNC) material when subjected to large plain strain deformation. The purpose of the model is to demonstrate its relevance to experimental results conducted on magnetically oriented reinforcements, and initial comparisons are made here too magnetically aligned nickel-coated short carbon fibres in a natural rubber matrix (at both small strain and large strain). The model is extended into a multiscale model and we demonstrate the large deflection of a reinforced beam with oriented platelets and the effects these orientations have on the maximum deflection of the beam. The results show that tailoring the platelet orientations can be used to achieve improved performance in devices such as microswimmers and actuators.

2. Large strain homogenised model

In the following, we consider the 2-D simplified Representative Volume Element (RVE) shown in Fig. 1 under the assumption of plane strain deformation. This assumptions is consistent with the actual geometry of reinforcements such as clays or graphene that have and with the platelets having one or two preferred directions. The ratio between the height H and the length L of the RVE is kept fixed for all simulations and equal to 1, i.e., square RVE. The ratio t between length and thickness of the platelet is $t = 40$ and corresponds to a volume fraction of 0.8 vol% that is typical of the values used in nanocomposites [9].

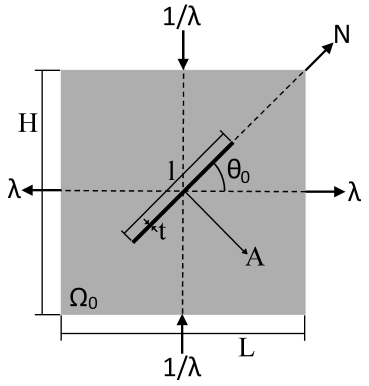

Figure 1. A representation of the applied boundary condition on the undeformed RVE.

Under the plane strain assumption, the overall deformation gradient $\overline{\mathbf{F}}$ applied to the RVE is

$$\overline{\mathbf{F}} = \begin{bmatrix} \overline{\lambda} & 0 & 0 \\ 0 & \overline{\lambda}^{-1} & 0 \\ 0 & 0 & 1 \end{bmatrix}. \tag{1}$$

Both the matrix and the filler are assumed to behave like incompressible neo-Hookean materials

with the strain energy functions given by

$$\Psi_\alpha(\mathbf{F}) = \frac{\mu_\alpha}{2}(I_1 - 3) - p_\alpha(I_3 - 1), \tag{2}$$

where $\alpha = F$ or M and μ_α is the shear modulus of the constituents. Here $I_1 = \text{tr}\{\mathbf{F}\mathbf{F}^T\}$ and $I_3 = \det\{\mathbf{F}\}$.

For the numerical simulations, the shear modulus of the matrix was $\mu_M = 1$ whereas the corresponding values for the filler were in the range $\mu_F = \{1, 10, 100, 1000\}$. p_α is indeed determined from the boundary conditions.

Parametric simulations were run with Abaqus 6.12 for different values of the material parameters of the constituents and orientation of the nanoplatelet $\theta_0 \in [0, 90]$. For each orientation the mesh was automatically generated through the Abaqus input file; the number of elements was established through a convergence check and it was seen that a good accuracy/convergence was reached with 3960 elements, with a moderate bias meaning more elements in and around the platelet/interface.

The periodic boundary conditions were enforced on the RVE through the Abaqus DISP subroutine. The effective incremental moduli are obtained by constructing the numerical tangent through a linear perturbation analysis after each step of the nonlinear analysis.

3. Identification of the overall constitutive response

When the particles are spherical shaped or have a preferred direction, but uniform orientation distribution, the overall behaviour of the composite is isotropic and the corresponding stress-strain relationship at the macroscale would follow the behaviour of the constituents. For a a neo-hookean incompressible material reinforced with rigid particles, Lopez-pamies et al. [10] have recently shown that the homogenised response is still neo-hookean incompressible.

Our case is subtlety different. The nanoplatelets are anisotropic with a principal direction given by the axis of the platelet itself. Therefore it is assumed that the overall behaviour of the composite would be transversely isotropic with the axis of isotropy given by the orientation of the platelet. This is indeed the case of composite whose fibres are oriented in a preferred direction.

The the overall constitutive strain energy function is hence assumed of the form:

$$\overline{\Psi}(\overline{I_1}, \overline{I_4}) = \frac{\mu}{2}\left[\overline{I_1} - 3 + \gamma(\overline{I_4} - 1)^2\right] - p(\overline{I_3} - 1) \tag{3}$$

where $\overline{I_4} = \overline{\mathbf{F}}^T\overline{\mathbf{F}} : \mathbf{N}\otimes\mathbf{N}$ is the standard anisotropic invariant that represents the stretch in the direction of the platelet. If θ_0 is the direction of the platelet in the undeformed configuration, then $\mathbf{N} = (\cos(\theta_0), \sin(\theta_0), 0)$ while the direction normal to the platelet is $\mathbf{A} = (-\sin(\theta_0), \cos(\theta_0), 0)$. The current normal vector $\mathbf{a}$ is $\mathbf{a} = \|\overline{\mathbf{F}}^{-T}\mathbf{A}\|^{-1}\overline{\mathbf{F}}^{-T}\mathbf{A}$, that in view of (1) gives the current orientation of the platelet θ in terms of the original angle θ_0:

$$\theta = \frac{\pi}{2} - \tan^{-1}\left[\frac{\overline{\lambda}^2}{\tan\theta_0}\right]. \tag{4}$$

The intent of our analysis is to show in what limit of the aspect ratio of the platelet and the size of the RVE the overall composite can be described as transversally isotropic. These models are usually employed to describe long fibre reinforced materials with the fibres spanning the entire length of the body. When the inclusion is actually shorter than the RVE one has to assess the predicting capabilities of these models against the numerical results.

4. Results and discussion

The inclusion of a stiff platelet reinforcement is expected to increase the overall stiffness of the RVE; whilst the transversely isotropic nature of the material means that the results are effected by the orientation of the platelet. For materials subject to large deformations, such as rubber, this transversely isotropic behaviour is expected to have significant effects upon the large strain behaviour due to the initial orientation of the platelet and its subsequent rotation as the RVE is stretched.

The results of the large strain analysis are shown in Fig. 2 for different orientations of the reinforcement, $\theta_0 = \{0°, 25°, 45°, 65°, 90°\}$, heterogeneity contrast, $\mu_F/\mu_M = 1000$, and maximum tensile stretch, $\bar{\lambda} = 1.6$. This latter value has been chosen because composites are very unlikely to be subjected to deformation larger than 50%.

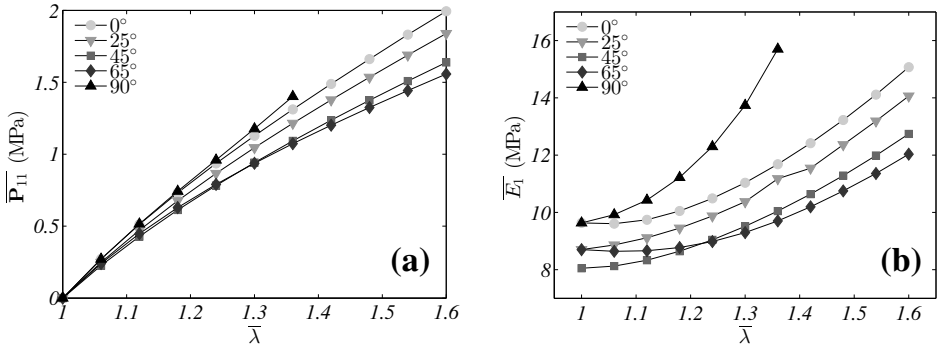

Figure 2. Nominal stress against stretch (a) and effective longitudinal modulus $\overline{E_1}$ (b) against stretch $\bar{\lambda}$ for different orientation of the reinforcement, $\theta_0 = \{0°, 15°, 45°, 65°, 90°\}$. In both cases $\mu_F/\mu_M = 1000$ and $AR = 40$ $vol = 0.8\%$.

The effect of the initial orientation θ_0 are apparent from Fig. 2a: 0° and 90° orientations confer to the RVE the higher stiffnesses whereas the 45° RVE has the softer response. In this configuration the stress applied on the boundary of the RVE is transferred by the platelet predominantly by shear forces, hence the softer response. The same behaviour is inferred by Fig. 2b where the longitudinal incremental moduli $\bar{E}_1$ is plotted against the stretch; at $\bar{\lambda} = 1$, i.e., the undeformed configuration, the corresponding values of $\bar{E}_1$ $\{9.63, 8.70, 8.05, 8.70, 9.63\}$ MPa. These results are indeed in accordance with the linear theory of laminate that predicts identical stiffnesses at 0° and 90° (and minimum stiffness at 45°). At larger stretches, however, the two curves diverges with the 90° RVE furnishing the stiffer response. Interestingly, the two complementary angles 25° and 65° have the same small strain longitudinal modulus but, as the stretch increases, the 65° one becomes softer and about at $\bar{\lambda} = 1.22$ is even softer than the 45° RVE.

This result illustrates the two distinct types of stiffening that the model shows: longitudinal

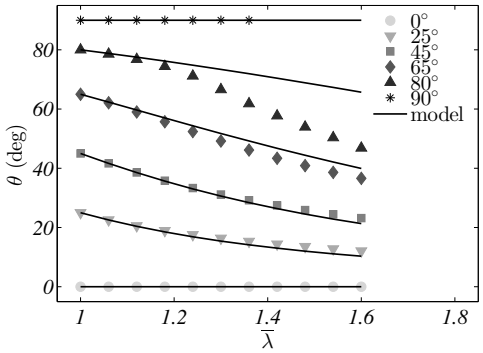

Figure 3. The platelet change of orientation during deformation for different configuration of the reinforcement $\theta_0 = \{0, 25, 45, 65, 90\}$ degrees and $\mu_F/\mu_M = 1000$ against Eq. (4).

stiffening due to a stress transfer from the matrix to the platelet (most prominent when the platelet is oriented parallel towards the loading axis i.e. $\theta_0 = 0°$), and lateral stiffening due to the Poisson's effect (when the platelet is oriented perpendicular to the loading direction i.e. $\theta_0 = 90°$). The fact that the stiffness at $\theta_0 = 90°$ is higher at large stretch than $\theta_0 = 0°$ (shown clearly in Fig. 2b) shows that the lateral stiffening effect is stronger at high stretch; however it is expected that the rotation of the platelet during stretching will have a significant effect upon the large strain behaviour of the material. This can be seen when comparing $\theta_0 = 90°$ and $\theta_0 = 65°$; in this latter case the initial oblique angle of the platelet allows it to rotate and decrease the Poisson's effect, thereby decreasing the lateral stiffening effect.

To further analyse these effects, the evolution of the platelet orientation in terms of the overall stretch $\bar{\lambda}$ has been plotted in Fig. 3 against Eq. 4. When the fibres span the entire RVE, Eq. (4) gives the exact expression of the current reinforcement angle; however in the present case, the movement of the platelet is not constrained to the boundary that causes Eq. 4 to give only approximate results with a larger error for larger angles. Apparently, due to the geometry of the RVE, at 0 and 90 degrees no reorientation of the platelet takes place. On the contrary, when the angle $\theta_0 >$ and $\theta_0 < 90$, the platelets aligns itself in the direction of the applied load, i.e., the 1-axis. For instance, the platelet initially oriented at 65 deg reaches the orientation of 45 deg at $\lambda = 1.3$ that corresponds to a rotation of about 20 deg. Interestingly during the deformation the RVE assesses the state of minimum stiffness that causes an effect in terms of the stress-strain curves, e.g., the tangent stiffness of the 65 deg RVE becomes softer than 45 deg ones.

Due to the geometry of the reinforcement, the overall response of the RVE is supposed to be orthotropic with the axis of transverse isotropy given by the orientation of the platelet. To validate this hypothesis the transverse isotropic model (2) is compared to the strain energy function as computed by Abaqus. The results of the comparison are shown in Fig. 4 where the strain energy function $\overline{\Psi}$ has been plotted against $\overline{I_1} - 3$ and $(\overline{I_4} - 1)^2$ for different hetereogenity contrast 10 (a), 100 (b) and 1000 (c). In all cases the linearity of the model with the two invariants is evident (all the points belong to the same plane).

The corresponding values of μ and γ in Eq. (3) are

$$\begin{aligned} \mu_{10} &= 2.020 \ \text{MPa}, & \gamma_{10} &= 0.143, \\ \mu_{100} &= 2.035 \ \text{MPa}, & \gamma_{100} &= 0.495, \\ \mu_{1000} &= 2.040 \ \text{MPa}, & \gamma_{1000} &= 0.598, \end{aligned}$$

that show the predominant effect of the inclusion rigidity on the parameter γ rather than μ. Indeed γ is a measure of the transverse isotropy of the RVE with $\gamma = 1$ corresponding to the isotropic neo-Hookean model. On the contrary the effect of the platelet stiffness on the equivalent modulus μ are rather limited due to the low volume fraction considered, i.e., *vol.%* = 0.8.

The accurate fit of the model confirms that overall behaviour of the RVE can be effectively modelled with the constitutive equation (3) and hence that the assumption of transverse anisotropy is acceptable for the considered platelet geometry.

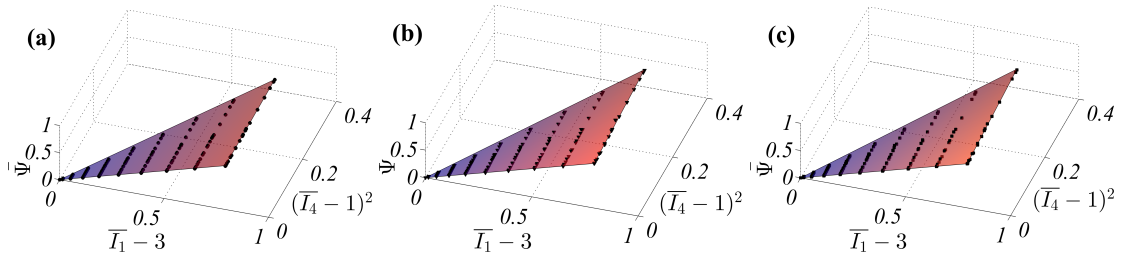

Figure 4. The transverse isotropy of the model is shown by the close fitting to Eq. (3). The planes show the constitutive model fitted to the data. The plotted dots show the numerical values of the strain energy function as computed by Abaqus. The corresponding values of stretches and angles are $\overline{\lambda} = [0.7, 1.6]$ and $\theta_0 = [0°, 90°]$.

4.1. Small strain response

Whilst the orientation of the platelet is important in determining the large strain results of the RVE, the small strain response of the material also shows very clearly the effect of the initial platelet orientation, θ_0, on the elastic modulus (Fig. 5). Interestingly, for the particular case considered, i.e., neo-Hookean constituents and RVE subjected to uniaxial extension, the platelet remains almost unstressed when oriented at 45°; this is mostly noticeable from the limited influence that the increase in the ratio μ_F/μ_M has on apparent tensile modulus of the composite with all the curves $\mu_F/\mu_M = \{1, 10, 100, 1000\}$ almost perfectly overlapping in Fig. 5a. At higher platelet orientations, $\theta_0 > 45°$, the lateral stiffening effect is in effect and is only very slightly decreased compared to the reciprocal angle below 45° (e.g. $0° \approx 90°$).

The primary mechanism for these two, almost equal, stiffening effects is unclear however the results of changing aspect ratio and vol.% show a very similar behaviour, this can be seen in Fig. 5. As would be expected, an aspect ratio of 1 gives an almost homogenous response (the slight inhomogeneity due to the square, rather than circular inclusion), whilst an increase in aspect ratio gives a larger stiffness at 0° and 90° due to the increased transverse isotropy (Fig. 5b). Similarly, increasing the vol.% of the platelet also increases the stiffness (Fig. 5c).

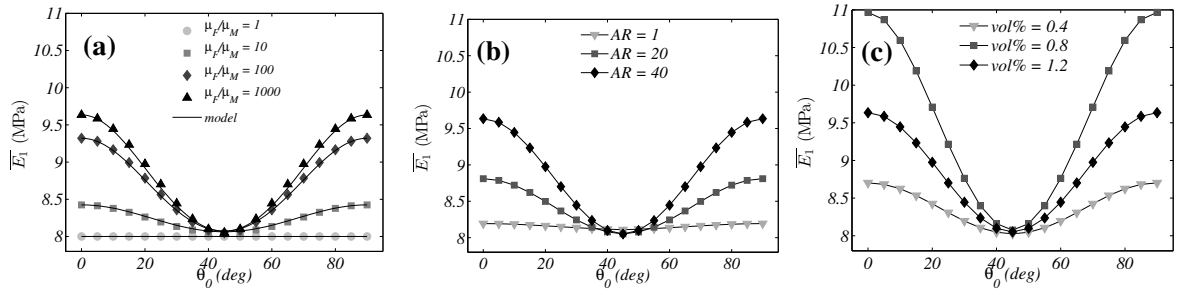

Figure 5. (a) The ratio μ_F/μ_M is shown to effect the stiffness, and vary with platelet orientation (AR = 40, $vol.\%$ = 0.8). (b) The aspect ratio is varied at a fixed vol.% of 0.8 and μ_F/μ_M = 1000. (c) The vol.% is varied at a constant AR of 40 and μ_F/μ_M = 1000.

5. Conclusions

An incompressible particle-reinforced neo-Hookean (IPRNC) material model subjected to large plain strain deformation has been developed. The addition of a rectangular nano-platelet reinforcement adds a transverse isotropy which is dependent on the orientation of the reinforcing platelet. In addition to an increased stiffness due to the aspect ratio and vol.% of the platelet, there are also two distinct stiffening effects: longitudinal and lateral. The longitudinal stiffening effect is usually seen in materials with some preferable orientation of anisotropic reinforcements, however the lateral stiffening effect is less well understood and documented although has been experimentally observed [11], and modelled for oriented CNTs [12] and continuous reinforcing fibres [10].

The numerical analysis carried out with Abaqus has shown a close match between the numerical computed strain energy function and the considered orthotropic neo-Hookean model. As a result, it is suggested that platelet reinforced composites are modelled as transversally isotropic solids when subjected to large plane strain deformations.

References

[1] R. R. Kohlmeyer and J. Chen. Wavelength-selective, ir light-driven hinges based on liquid crystalline elastomer composites. *Angew Chem Int Ed Engl*, 52(35):9234–7, 2013.

[2] W. Gao, X. Feng, A. Pei, C. R. Kane, R. Tam, C. Hennessy, and J. Wang. Bioinspired helical microswimmers based on vascular plants. *Nano Letters*, 14(1):305–10, 2014.

[3] P. Fratzl. Bone fracture: When the cracks begin to show. *Nat Mater*, 7(8):610–2, 2008.

[4] Brian R. Lawn, James J. W. Lee, and Herzl Chai. Teeth: Among nature's most durable biocomposites. *Annual Review of Materials Research*, 40(1):55–75, 2010.

[5] Peter Fratzl and Richard Weinkamer. Nature's hierarchical materials. *Progress in Materials Science*, 52(8):1263–1334, 2007.

[6] R. M. Erb, R. Libanori, N. Rothfuchs, and A. R. Studart. Composites reinforced in three dimensions by using low magnetic fields. *Science*, 335(6065):199–204, 2012.

[7] Tsunehisa Kimura, Yusuke Umehara, and Fumiko Kimura. Fabrication of a short carbon fiber/gel composite that responds to a magnetic field. *Carbon*, 48(14):4015–4018, 2010.

[8] N. Kitamura, K. Fukumi, K. Takahashi, I. Mogi, S. Awaji, and K. Watanabe. Orientation of carbon nano-fiber in carbon/silica composite prepared under high magnetic field. *IOP Conference Series: Materials Science and Engineering*, 18(5):052008, 2011.

[9] D. C. Stanier, A. J. Patil, C. Sriwong, S. S. Rahatekar, and J. Ciambella. The reinforcement effect of exfoliated graphene oxide nanoplatelets on the mechanical and viscoelastic properties of natural rubber. *Composites Science and Technology*, 95:59–66, 2014.

[10] Oscar Lopez-Pamies, Martín I. Idiart, and Zhiyun Li. On microstructure evolution in fiber-reinforced elastomers and implications for their mechanical response and stability. *Journal of Engineering Materials and Technology*, 133(1):011007, 2011.

[11] D. C. Stanier, S. Rahatekar, A. J. Patil, and J. Ciambella. Magnetically tailoring the short fibre reinforcement of natural rubber. *RubberCon 2014*. (to appear).

[12] Giovanni Formica, Walter Lacarbonara, and Roberto Alessi. Vibrations of carbon nanotube-reinforced composites. *Journal of Sound and Vibration*, 329(10):1875–1889, 2010.